Evaluating the emissions and performance of two dual-mode RCCI combustion strategies under the World Harmonized Vehicle Cycle (WHVC)

Energy Conversion and Management, Volume 149, 1 October 2017, Pages 263-274.
http://dx.doi.org/10.1016/j.enconman.2017.07.034

Antonio García[a,*], Javier Monsalve-Serrano[a], Vinícius Rückert Roso[b], Mario Eduardo Santos Martins[c]

[a]CMT - Motores Térmicos, Universitat Politècnica de València, Camino de Vera s/n, 46022 Valencia, Spain
[b]CTM – Centro de Tecnologia da Mobilidade, Universidade Federal de Minas Gerais, Belo Horizonte, MG, Brazil
[c]Grupo de Pesquisa em Motores, Combustíveis e Emissões, Universidade Federal de Santa Maria, Santa Maria, RS, Brazil

Corresponding author (*):
Dr. Antonio García (angarma8@mot.upv.es)
Phone: +34 963879659
Fax: +34 963877659

Abstract

This work compares the emissions and performance of two dual-mode reactivity controlled compression ignition (RCCI) combustion strategies under the World Harmonized Vehicle Cycle (WHVC), a chassis dynamometer version of the World Harmonized Transient Cycle (WHTC) test proposed by the EURO VI emission regulation for heavy-duty engines. The major difference between the two dual-mode combustion strategies investigated is that, while one of them relies on covering with conventional diesel combustion (CDC) the part of the map that cannot be covered by RCCI regime (RCCI/CDC dual-mode), the other does it relying on dual-fuel diffusion combustion (dual-mode dual-fuel).

The influence of the gear shifting strategy on the emissions and performance over the WHVC is discussed first. Later, both dual-mode concepts are compared considering the optimal gear shifting strategy. The results suggest that dual-mode dual-fuel concept allows reducing the specific fuel consumption by 7% in average versus RCCI/CDC concept. Moreover, NO_x emissions are around 87% lower with dual-mode dual-fuel, meeting the EURO VI requirements without the need for an SCR aftertreatment system. In counterpart, HC and CO emissions are near 2 and 10 times greater, respectively, for dual-mode dual-fuel than for RCCI/CDC.

Keywords

Reactivity controlled compression ignition; Dual-fuel combustion; Dual-mode concept; EURO VI emissions; Engine cycle simulation

1. Introduction

Consumption of petroleum products in the European Union (EU) increased by 13% between 1990 and 2005. This trend was mainly driven by the fuel consumption of transportation sector. Between 2005 and 2012, the oil consumption decreased in all sectors due to the recession, but transport sector experienced the smallest decrease by

only 8%. In fact, in 2012 the transport industry had 76% share of the petroleum consumption in the EU, of which near 74% belonged to road transport. This means that internal combustion engines (ICE) for transportation are responsible of near 60% of the energy consumption of petroleum products in Europe [1].

Engine and vehicle manufacturers are continuously working on developing new technologies [2] to increase fuel economy and reduce pollutant emissions [3][4] according to requirements imposed by both users and regulations [5]. Historically, the higher efficiency of compression ignition (CI) engines than spark ignition (SI) engines has led them to lead heavy-duty transportation. However, in spite of conventional diesel combustion (CDC) offers high efficiency, it requires using complex and costly exhaust aftertreatment systems to reach the NO_x and soot emissions levels imposed by the currently in force EURO VI regulation. The technological solution adopted by the majority of heavy-duty engine manufacturers for moving from EURO V to EURO VI regulation is quite similar [6]. It consist of a two-stage NO_x reduction; exhaust gas recirculation (EGR) first, followed by selective catalytic reduction (SCR) exhaust aftertreatment, and diesel particulate filter (DPF) to remove particulates [7]. Unburned hydrocarbons (HC) and carbon monoxide (CO) emissions are reduced using a diesel oxidation catalyst (DOC). As a result of the modifications introduced to fulfill the different regulatory stages, a EURO VI heavy-duty vehicle equipped with a 12 liter engine has experienced an increase of approximately 6000 € as compared to its EURO II equivalent [8].

Considering this scenario, the research community is working on developing alternative combustion concepts that allow high efficiency and low NO_x and soot emissions simultaneously, thus contributing to reduce the aftertreatment necessities. In this sense, different low temperature combustion (LTC) strategies such as the homogeneous charge compression ignition (HCCI) [9], premixed compression ignition (PCI) [10], diesel partially premixed combustion (PPC) [11], gasoline PPC [12] and PPC spark assisted [13][14] have been studied up to date. These strategies base on promoting an air-fuel premixed environment before the start of combustion by injecting the fuel in the early instants of the compression stroke and high EGR levels, which results in extended ignition delay periods and low local flame temperatures. However, the use of a single fuel confines the operating region to a very narrow range, either because of excessive pressure gradients or due to misfire conditions.

The dual-fuel LTC concept so-called Reactivity controlled compression ignition (RCCI) has been deeply investigated over the last decade [15]. This combustion concept can be easily implemented by adding a port fuel injector (PFI) to a CI engine to inject a second fuel with different reactivity than that injected directly into the combustion chamber [16]. Experimental and simulation studies have demonstrated that RCCI is capable of achieving diesel-like or better efficiency [17] together with near-zero NO_x [18] and soot emissions [19][20]. To achieve this, the effect of different variables on RCCI efficiency and emissions has been deeply investigated. In this sense, the engine settings [21][22], piston geometry [23], compression ratio [24], fuels used [25][26], auxiliary systems [27] and air management conditions [28] have been optimized. The majority of the investigations found in literature rely on RCCI to achieve NO_x values in steady-state conditions below EURO VI regulation (0.4 g/kWh) and soot emissions in the range of 0.1-0.2 FSN [29]. These results would confirm the great potential of the RCCI concept,

meaning that near 60% of the total aftertreatment costs of heavy-duty vehicles could be reduced by removing the selective catalytic reduction (SCR) system [8]. However, these emissions constraints can be only fulfilled in a certain portion of the engine map [30], thus requiring the implementation of a dual-mode concept to cover the whole engine operating range.

Previous investigations have demonstrated the capabilities of two dual-mode RCCI concepts in steady-state operation, dual-mode RCCI/CDC [31] and dual-mode dual-fuel (DMDF) [32]. The major difference between these combustion strategies is that, while one of them relies on covering with conventional diesel combustion the part of the map that cannot be covered by RCCI regime, the other does it relying on dual-fuel diffusion. Both strategies have shown clear potential over the world harmonized stationary cycle (WHSC), in which NO_x emissions, urea consumption and diesel particulate filter (DPF) regeneration were substantially reduced versus CDC operation. The objective of the current work is to compare the potential of both combustion modes in transient conditions, also required by the EURO VI type approval process. For this purpose, performance and emissions of both dual-mode concepts are evaluated over the World Harmonized Vehicle Cycle (WHVC) [33], a chassis dynamometer test developed based on the same set of data used for the development of the World Harmonized Transient Cycle (WHTC) [34], defined in the EURO VI regulation [35]. Cycle simulations were carried out using a dedicated vehicle model and steady-state experimental maps of emissions and performance. Before performing the direct comparison, the effect of seven different gear shifting strategies is analyzed. Later, both dual-mode combustion concepts are compared using the optimum gear shifting strategy, analyzing their differences in terms of emissions and performance.

2. Materials and methods

2.1. Test cell characteristics and engine description

Engine tests were carried out in a single-cylinder medium-duty EURO VI diesel engine, whose main characteristics are depicted in table 1. The dual-mode RCCI/CDC was implemented using the stock compression ratio (17.5:1), while to develop the dual-mode dual-fuel, the engine CR was reduced down to 15.3:1 by means of the piston bowl modification. The piston bowl geometry was designed following the guidelines found in previous researches [33][37].

Table 1. Engine characteristics.

Style	4 Stroke, 4 valves, direct injection
Manufacturer / model	VOLVO / D5K240
Maximum in-cylinder pressure	190 bar
Bore x Stroke	110 mm x 135 mm
Connecting rod length	212.5 mm
Crank length	67.5 mm
Unitary displaced volume	1275 cm^3
Compression ratio (nominal)	17.5:1
Compression ratio for RCCI	15.3:1

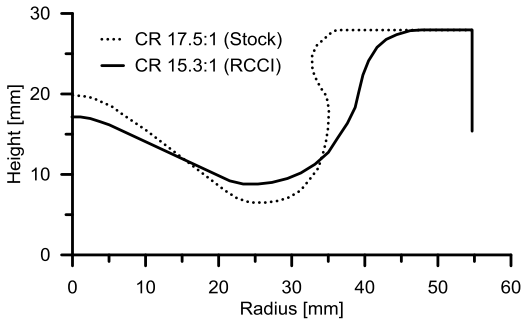

Figure 1. Cross sectional view of the stock (CR 17.5:1) and RCCI (CR 15.3:1) piston geometries.

As shown in Figure 2, the SCE was built on the base of the production Volvo D5K240 multi-cylinder engine by isolating one cylinder. The remaining cylinders work in CDC regime controlled by the ECU to balance the cylinder-to-cylinder pressure peaks. This engine layout makes not possible to isolate torque measurements from the SCE, so that values acquired from the experiments are provided in indicated basis. The figure shows that both sides of the engine (SCE and other cylinders) are fully instrumented. To isolate the SCE side, the stock air-loop was replaced by different elements such as the screw compressor, dryer, heater and settling chamber to allow a full control during the engine tests. Same job was done in the exhaust line, where a backpressure valve was installed to reproduce the backpressure generated by the turbine in the stock configuration. Moreover, an additional air-loop was designed to redirect the EGR flow to the intake line. Gaseous emissions were sampled at the end of the exhaust line using a five gas Horiba MEXA-ONE-D1-EGR analyzer. Emissions samples were averaged during 40 seconds once achieved steady-state conditions. Smoke emissions were measured using an AVL 415S Smoke Meter. In this case, three samples of a 1 liter volume each with paper-saving mode off were acquired for each operating point. The accuracy of the different devices used to acquire data is summarized in table 2.

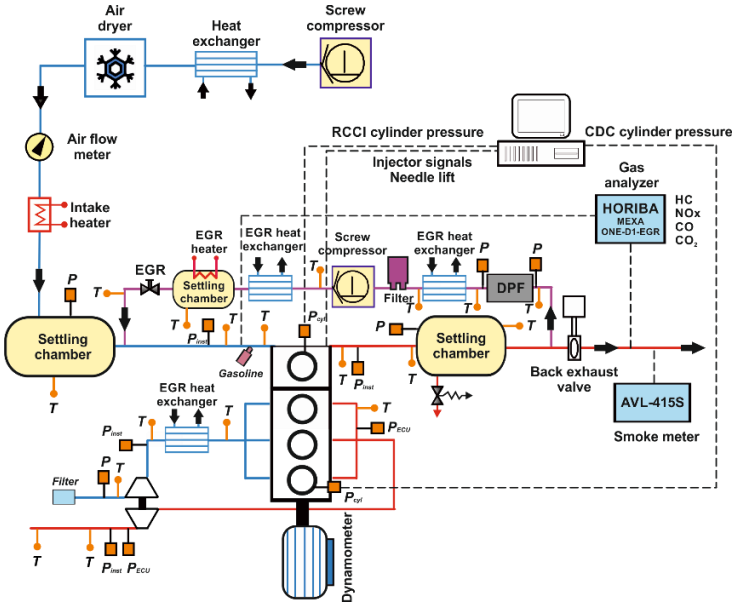

Figure 2. Test cell layout.

Table 2. Accuracy of the instrumentation used in the experimental work.

Variable measured	Device	Manufacturer / model	Accuracy
In-cylinder pressure	Piezoelectric transducer	Kistler / 6125C	±1.25 bar
Intake/exhaust pressure	Piezorresistive transducers	Kistler / 4045A10	±25 mbar
Temperature in settling chambers and manifolds	Thermocouple	TC direct / type K	±2.5 °C
Crank angle, engine speed	Encoder	AVL / 364	±0.02 CAD
NO_x, CO, HC, O_2, CO_2	Gas analyzer	HORIBA / MEXA-ONE-D1-EGR	4%
FSN	Smoke meter	AVL / 415S	±0.025 FSN
Gasoline and diesel fuel mass flow	Fuel balances	AVL / 733S	±0.2%
Air mass flow	Air flow meter	Elster / RVG G100	±0.1%

Two injection systems were used to implement the dual-fuel concept. The diesel fuel was injected using the stock solenoid injector and common-rail system. However, the stock ECU was replaced by an in-house developed Drivven controller to allow the calibration work. The main characteristics of the diesel injection hardware are depicted in table 3. An additional fuel injection system was installed to inject the low reactivity fuel by port fuel injection (PFI). The port fuel injector was located at the intake manifold, 160 mm far from the intake valves. The PFI timing was set 10 CAD after the intake valve opening (IVO) to allow the fuel to flow to the combustion chamber without introducing variability due to valve wetting. The main characteristics of the PFI system are summarized in table 3.

Table 3. Details of the direct and port fuel injection systems.

Direct injector		Port fuel injector	
Actuation Type	Solenoid	Injector Style	Saturated
Steady flow rate @ 100 bar [cm^3/min]	1300	Steady flow rate @ 3 bar [cm^3/min]	980
Included spray angle [°]	150	Included Spray Angle [°]	30
Number of holes	7	Injection Strategy	single
Hole diameter [µm]	177	Start of Injection [CAD ATDC]	340
Maximum injection pressure [bar]	2000	Maximum injection pressure [bar]	5.5

The fuels used for mapping both dual-mode combustion concepts were optimized in each case considering previous works [22][26]. The dual-mode RCCI/CDC engine map was completed using diesel B7 (diesel fuel with 7% of biodiesel content by volume form Vegetable Oil Methyl Esters) and E20-95 (fuel blend containing 80% of 95 octane number gasoline and 20% of ethanol content by volume) as high and low reactivity fuels, respectively, while the dual-mode dual-fuel mapping was done using regular diesel and 95 octane number gasoline. The main properties of the fuels are shown in table 4.

Table 4. Main properties of the fuels used in both dual-mode concepts.

	Diesel B7	E20-95	Diesel	Gasoline
Density [kg/m^3] (T= 15 °C)	837.9	745	824	720
Viscosity [mm^2/s] (T= 40 °C)	2.67	-	2.8	-
RON [-]	-	99.1	-	95
MON [-]	-	85.6	-	85
Biodiesel content [% by volume]	7	-	<0.2	-
Ethanol content [% by volume]	-	19.7	-	-
Cetane number [-]	54	-	51	-
Lower heating value [MJ/kg]	42.61	40.05	42.92	42.4

2.2. Dual-mode combustion strategies description

The dual-mode combustion approach relies on switching between different combustion strategies to achieve clean and efficient operation along the whole engine map. In this sense, diesel-like or better gross indicated efficiency (GIE), together with simultaneous ultra-low NO_x and soot emissions are sought during the engine experiments. Mandatory constraints to keep the operating points as valid during the engine mapping were to ensure maximum pressure rise rates (PRR) and in-cylinder pressure peaks (P_{max}) below 15 bar/CAD and 190 bar, respectively.

Figure 3 shows the two dual-mode concepts studied in this paper. The dual-mode RCCI/CDC was implemented using the stock compression ratio (17.5:1) to allow high efficiency in the CDC parts of the map. This high CR resulted in very narrow RCCI range, from 4 to 9 bar roughly. Engine operation below 4 bar was limited by excessive unburned products (CO >5000 ppm) while the upper part of the map was restricted by excessive pressure gradients (PRR >15 bar/CAD). These operating regions were completed with CDC regime. Fuels used were diesel B7 and E20-95 as high and low reactivity fuels, respectively. The ethanol-based low reactivity fuel (LRF) was selected to compensate partially the high CR through its greater ON and enthalpy of vaporization, which allows reducing the intake charge temperature at the intake valve closing (IVC). It is interesting to remark that, in spite of the narrow region covered by RCCI regime, it contains the weightiest points of the world harmonized stationary cycle (WHSC). This leads to a potential reduction of 9% in urea mass, and halve the diesel particulate filter (DPF) regeneration needs when compared to single CDC operation. Full details about the engine mapping procedure and specific settings for the dual-mode RCCI/CDC are provided in [29].

With the aim of increasing the dual-fuel operating region in the map, the engine CR was reduced down to 15.3:1 by means of the piston bowl modification (Figure 1). With this configuration, the dual-mode dual-fuel combustion mode was developed. This dual-mode strategy is based on using two combustion regimes to cover the engine map, RCCI and diffusive dual-fuel. Both regimes rely on the dual-fuel combustion concept, but major difference between them is that RCCI is intended to achieve ultra-low NO_x and soot emissions, while the emissions limits are more relaxed in the case of dual-fuel diffusion. Dual-fuel diffusion is applied when RCCI regime gets restricted by excessive PRR (at high load), so that the emissions and performance references to be achieved in

this region are those found during CDC combustion. As depicted in Figure 3, a single diesel pulse near top dead center (TDC) is used to avoid excessive PRR in this region.

The RCCI regime is divided in two combustion strategies considering the injection strategy proposed, fully and highly premixed. The two advanced diesel injection pulses used in the fully premixed RCCI strategy lead to a high efficiency HCCI-like combustion, with NO_x and soot emissions below 0.4 g/kWh and 0.2 FSN, respectively. As load increases, diesel injection strategy is modified to avoid excessive PRR, leading to the highly premixed RCCI strategy. In particular, the second diesel pulse is shifted towards TDC to allow a more sequential autoignition. While NO_x emissions are still maintained below 0.4 g/kWh in this case, soot levels are generally increased, showing peaks of 1 and 1.2 FSN in some operating conditions. This occurs because the mixing time reduction of the second diesel injection. The complete details about the engine mapping procedure and specific settings for the dual-mode dual-fuel concept can be found in [32].

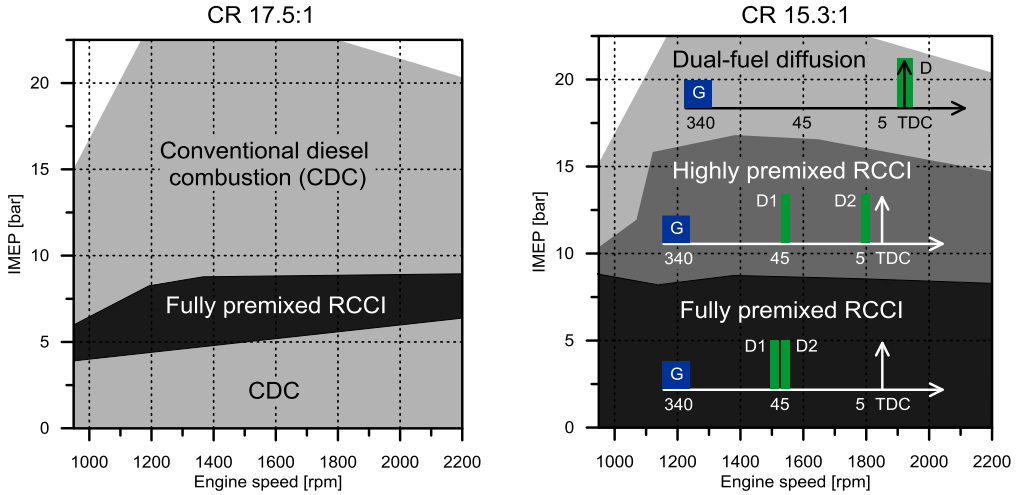

Figure 3. Injection-combustion strategies used to cover the engine map with the two dual-mode studied: dual-mode RCCI/CDC (left) and dual-mode dual-fuel (right) [32].

2.3. Modelling procedure

In order to evaluate the performance of the two dual-mode RCCI combustion strategies when applied to a vehicle under the World Harmonized Vehicle Cycle (WHVC), a one dimensional computer model was developed with GT-Suite software from Gamma Technologies®. The vehicle chosen was a FL240 series light truck made by Volvo, with the specifications as shown in table 5.

Table 5. Vehicle Characteristics.

Vehicle Mass [kg]	7500
Vehicle Drag Coefficient [-]	0.5
Frontal Area [m²]	6
Tires Size [mm/%/inch]	245/70/R17.5
Vehicle Wheelbase [m]	5
Final Drive Ratio [-]	3.73
Gear Ratio 1st [-]	6.75
Gear Ratio 2nd [-]	3.6
Gear Ratio 3rd [-]	2.12
Gear Ratio 4th [-]	1.39
Gear Ratio 5th [-]	1
Gear Ratio 6th [-]	0.78

In this model, the differential equations of motion for the driveline components and the vehicle are integrated in time, calculating transient speeds and torques in the system. Engine brake mean effective pressure (BMEP) input data was calculated using indicated and friction experimental data and correlated to engine speed and accelerator position. Maps of emissions, air and fuel consumption from the engine dynamometer were used to determine emissions and fuel consumption in steady state conditions [29][32] as a function of load and speed. Then, differential equations of vehicular motion were integrated in time, calculating transients of speed and torque and interpolating emissions and fuel consumption according to the load point demanded by the drive cycle condition. Rolling resistance was calculated by the model as a function of drag coefficient, rolling friction, and road grade are included in equation 1, which calculates the torque required for vehicle motion.

$$\tau_{vehicle} = \left[I_{trans1} + \frac{I_{trans2}}{R_t^2} + \frac{I_{dsh}}{R_t^2} + \frac{I_{axl}}{(R_d^2)(R_t^2)} + \frac{(M_{veh})(r_{whl}^2)}{(R_d^2)(R_t^2)}\right]\frac{d\omega_{drv}}{dt} - \left[\frac{I_{trans2}}{R_t^3} + \frac{I_{dsh}}{R_t^3} + \frac{I_{axl}}{(R_d^2)(R_t^3)} + \frac{(M_{veh})(r_{whl}^2)}{(R_d^2)(R_t^3)}\right]\omega_{drv}\frac{dR_t}{dt} + \left[\frac{F_{aer} + F_{rol} + F_{grd}}{R_d R_t}\right] r_{whl} \quad (1)$$

The first term of equation represents the torque required to accelerate the effective inertia, evaluated at the clutch of the entire drivetrain. On this, I_{trans1} and I_{trans2} present the inertia in the input and output of transmission system, respectively. Likewise, I_{dsh} and I_{axl} are driveshaft and axle moment of inertia. These terms relate the number of axles and inertia of each wheel, adapted to the vehicle characteristics. R_d and R_t are terms of final drive and transmission ratio for each gear. Vehicle speed (ω_{drv}) at the instant of time (t) is directly related to the wheel radius (r_{whl}) and vehicle mass (M_{veh}). The second term of equation 1 represents the load induced by a transient gear ratio, where the vehicle object internally creates a transmission model based on the information of vehicle transmission references. External forces on vehicle are added in

the third term as aerodynamic forces (F_d), rolling resistance forces (F_{rol}) and gravity forces (F_{grd}) [38].

The driving cycle used was the World Harmonized Vehicle Cycle (WHVC), which is a chassis dynamometer test based on the World Harmonized Transient Cycle (WHTC). Since WHVC is not a standardized test such as WHTC, the results can be used only to compare the respective vehicle and engine emission levels for research purposes [39]. As shown in Figure 4, the total duration of the WHVC test is divided in three segments, representing conditions of urban driving (first 900 s with average and maximum speeds of 21.3 km/h and 66.2 km/h, respectively), rural driving (following 481 s with average and maximum speeds of 43.6 km/h and 75.9 km/h) and motorway driving (last 419 s with average and maximum speeds of 76.7 km/h and 87.8 km/h).

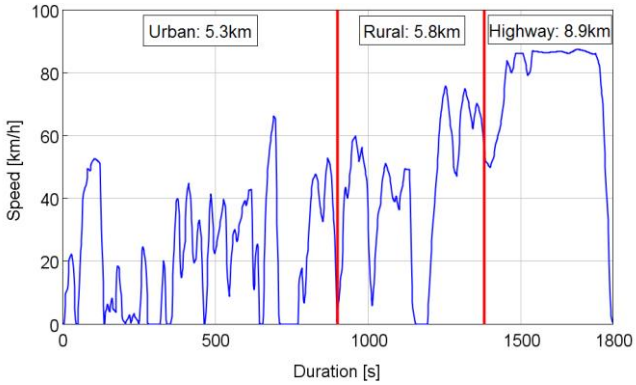

Figure 4. World Harmonized Vehicle Cycle (WHVC) [40].

In order to compare the influence of both combustion strategies on emissions and fuel consumption in the WHVC, two models were built with the same characteristics of vehicle and driver behavior, changing the input data related to emissions and performance accordingly. Figure 5 shows the logical representation of the model used, connecting the various components of the system and their submodels.

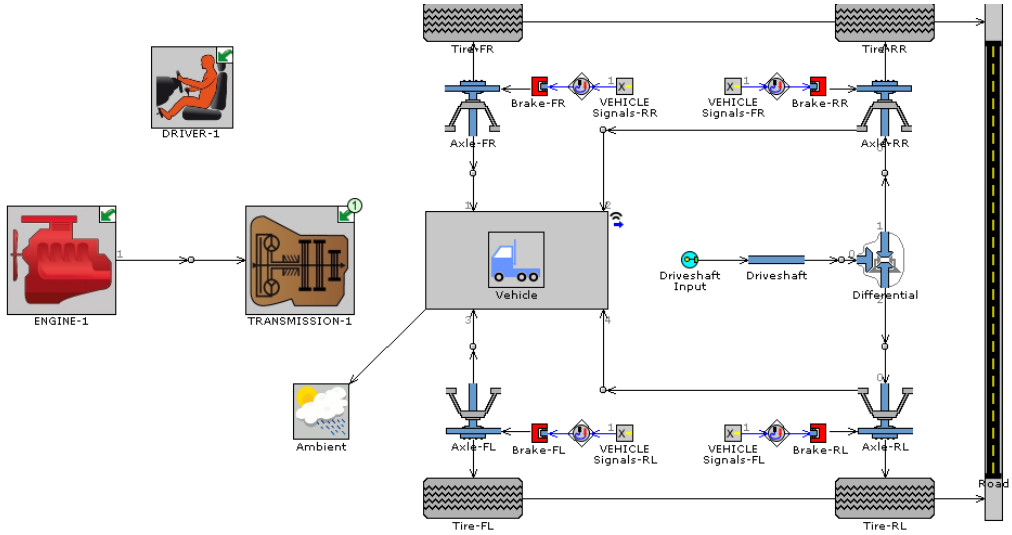

Figure 5. Vehicle model in GT-Suite software.

Gear shifting strategy has a large influence on engine speed and load, changing the permanence time in each region of the maps used. Thus, considering the baseline engine power and torque curves presented in Figure 6, seven operating ranges were simulated

to establish the best gear shifting strategy (points of up and down gear shifts). The seven strategies are summarized in Figure 7, in which the shadowed regions represent the engine speed range covered by each strategy. From the seven strategies, strategy 3 provides conditions for maximum torque and strategy 4 for maximum power. The remaining five strategies are intermediate cases.

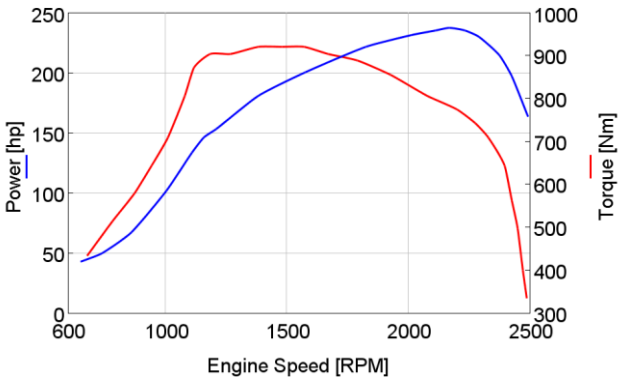

Figure 6. Power and torque curves for baseline engine [41].

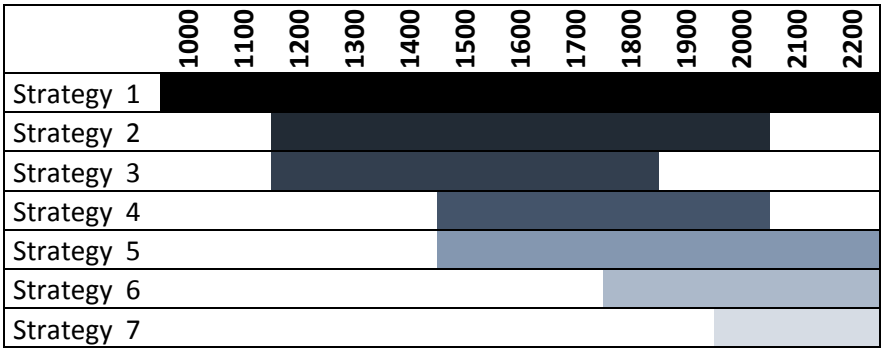

Figure 7. Seven gear shifting strategies evaluated. The shadow regions represent the engine speed range covered by each strategy.

3. Results and discussion

In order to analyze both dual-mode RCCI combustion strategies under the World Harmonized Vehicle Cycle (WHVC), results are presented referring to DMDF and RCCI/CDC data. Data from the concept that relies conventional diesel combustion to cover the part of the map that cannot be covered by RCCI will be referred as RCCI/CDC, while data from the dual-fuel diffusion concept will be referred as DMDF (Dual-mode dual-fuel). The results of the current investigation are divided in two subsections. The first subsection is dedicated to evaluate the seven operation ranges presented in Figure 7 to establish the best gear shifting strategy for both dual-mode combustion concepts. The second subsection shows specific emissions and fuel consumption according to operation points in the engine maps. Values for fuel and emission rates during the driving cycle are also presented in this subsection.

3.1. Gear shift strategy

This section presents results of gear shifting strategies to optimize fuel consumption and exhaust emissions for DMDF and RCCI/CDC combustion strategies. Table 6 summarizes

the simulation results for the seven operation ranges shown in Figure 7. All the simulated ranges were capable to reach the vehicle velocity needed to cover the WHVC driving cycle. Both combustion concepts were evaluated individually by establishing the best gear shifting points for each. In addition to specific values of emissions and fuel consumption, the total mass consumption of urea to meet EURO VI requirements was also considered. In this sense, since the urea needed to reduce 1 g/kWh of NO_x emissions can be estimated as being 1% of the fuel consumed [42], the urea required to reduce engine-out NO_x emissions up to EURO VI target (0.46 g/kWh) can be estimated as shown in equation 2.

$$m_{urea} = \left(NOx_{engine-out} - NOx_{Euro\,VI}\right) \cdot 0.01\, m_{diesel} \quad (2)$$

Table 6. Specific emission and fuel consumption for the seven gear shifting strategies in DMDF and RCCI/CDC dual-mode combustion strategies.

Operation Ranges		Combustion Strategy	BSFC (g/kWh)	BSNO$_x$ (g/kWh)	BSHC (g/kWh)	BSCO (g/kWh)	BSSoot (g/kWh)	Total Mass of Urea (g)
1000	**2200**		227.24	0.34	8.68	39.83	0.02	0.00
1200	**2000**		222.15	0.34	8.33	36.86	0.02	0.00
1200	**1800**		213.87	0.33	7.79	33.67	0.02	0.00
1500	**2000**	**DMDF**	232.70	0.41	8.35	39.41	0.02	0.00
1500	**2200**		232.70	0.41	8.35	39.41	0.02	0.00
1800	**2200**		228.10	0.70	4.81	30.51	0.07	5.75
2000	**2200**		224.17	0.83	3.61	24.54	0.10	8.16
1000	**2200**		235.86	2.12	3.48	3.83	0.02	40.10
1200	**2000**		236.27	2.14	3.49	3.84	0.02	40.47
1200	**1800**		230.17	2.52	3.31	3.64	0.01	48.47
1500	**2000**	**RCCI/CDC**	241.51	2.93	3.13	3.55	0.02	61.07
1500	**2200**		244.39	2.15	3.48	3.97	0.02	41.85
1800	**2200**		247.88	6.10	1.02	1.40	0.01	141.56
2000	**2200**		251.49	7.93	0.67	0.93	0.01	170.32

The already known potential of DMDF concept is an expressive reduction of NO_x emissions levels [32]. Then, it is expected that a small portion of urea is needed to meet homologation requirements. With this consideration, operation ranges of 1800-2200 rpm and 2000-2200 rpm were discarded for DMDF concept. The condition of maximum engine power (1500-2000 rpm) presented the highest values of brake specific fuel consumption (BSFC) if compared with other 6 cases. Best specific emission and fuel consumption values for DMDF concept are observed for the condition of maximum engine torque (1200-1800 rpm).

Lower mass of urea needed to meet the requirements are noticed in the highest ranges of engine operation (1000-2200 rpm and 1200-2000 rpm) for RCCI/CDC concept. However, lower values for NO_x, HC, CO and Soot specific emissions are observed in different ranges of engine operation. This behavior can be attributed to the different combustion characteristics observed in RCCI mode and CDC mode. Condition of

maximum engine torque (1200-1800 rpm) results in balanced emission values for the different exhaust gases and also the lower BSFC between the evaluated cases.

With better specific values for DMDF and balanced results for RCCI/CDC, the next subsection will present a comparison of emissions and performance considering the range of maximum engine torque (Strategy 3 - 1200-1800 rpm) for both dual-mode combustion strategies.

3.2. Emissions and performance comparison

This section evaluates the potential of both dual-mode combustion strategies considering the operation in the range of maximum torque, as established in section 3.1, with regards to BSFC and engine-out emissions. Engine maps from Figure 8 to Figure 12 correspond to experimental data from previous works [31][32], while the points in these figures present the operation points simulated for each dual-mode concept during the WHVC. Condition in each segment of the driving cycle can be observed according to the symbol used for the operation points. White dashed lines across the maps represent the boundaries of the different combustion strategies applied (Figure 3). It is possible to see that operation points for RCCI/CDC and DMDF are a bit different due to their individual combustion characteristics.

The operation points of both combustion strategies express that in a significant percentage of the WHVC driving, the simulated engine loads are below 10 bar IMEP. Optimal values for emissions and BSFC are observed if operating inside the blue region of the maps.

Figure 8 shows the simulated operation points within the experimentally acquired BSFC maps for both combustion concepts. It can be seen that, under the same shifting strategy (Strategy 3 in Figure 7), DMDF operation results in greater number of operating points performing closer to the optimum BSFC values. This will potentially lead to more efficient operation.

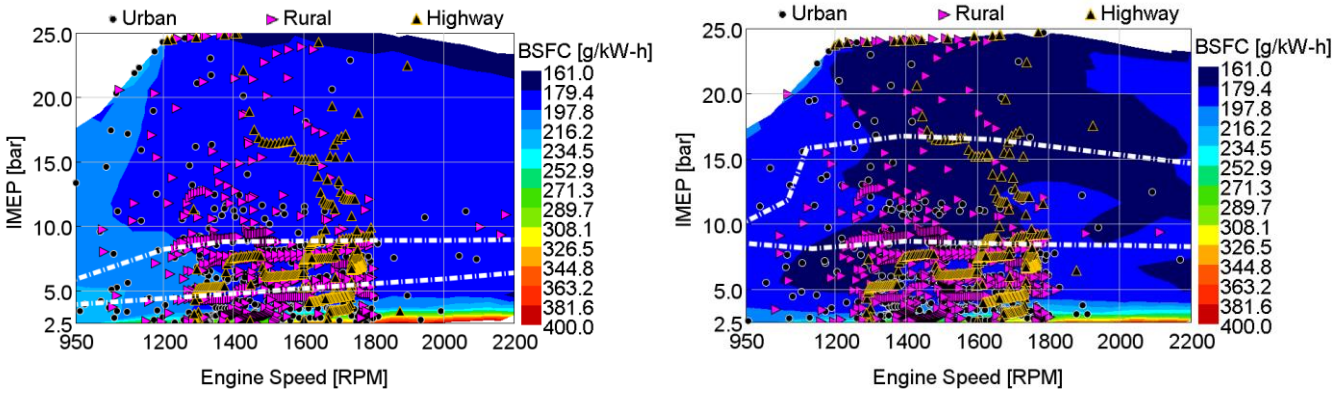

Figure 8. Operation points in specific fuel consumption map for RCCI/CDC concept (left) and DMDF concept (right).

Although the NO_x emissions behavior is quite similar for both cases (Figure 9), DMDF concept presents lower maximum values than RCCI/CDC. Thus, the average $BSNO_x$ is around 87% lower in DMDF strategy, yielding an average value of 0.33 g/kWh. Therefore, it proves the potential reduction of NO_x emissions as described by Benajes et al. [32], meeting the EURO VI requirements of 0.46 g/kWh [35] without the need for an

SCR aftertreatment system. In addition, the effectiveness of RCCI combustion in reducing NO_x emissions can be also observed in the left side of Figure 9, where the lowest emissions range is inside of RCCI operation region. Despite of it, a large portion of the operation is observed outside of RCCI region, being under CDC. In DMDF concept, however, the majority of the operation is covered by RCCI strategy, ranging from fully to highly-premixed RCCI combustion.

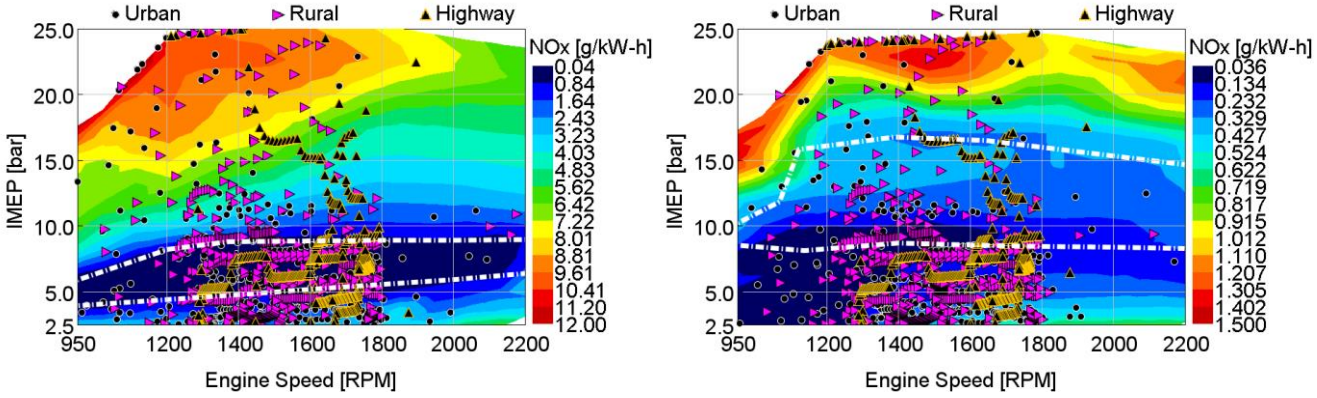

Figure 9. Operation points in NO_x emission map for RCCI/CDC concept (left) and DMDF concept (right).

A similarity between maps of HC and CO engine emissions is observed in Figure 10 and Figure 11. CO emissions follow the general diesel engine behavior and are the lowest with CDC at mid to high loads. DMDF also shows low values at high loads. However, for both CO and HC emissions, DMDF combustion shows higher values than RCCI/CDC, being more than 9 times higher in the case of CO, especially in low loads and mid-range speed. RCCI/CDC combustion shows higher values in mid-range engine speeds and loads, where the RCCI combustion prevails over CDC.

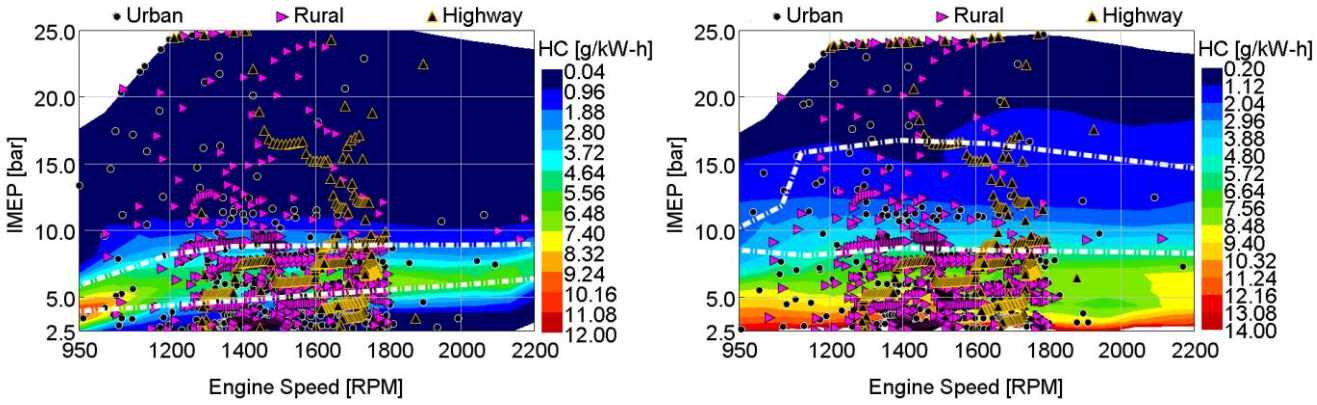

Figure 10. Operation points in HC emission map for RCCI/CDC concept (left) and DMDF concept (right).

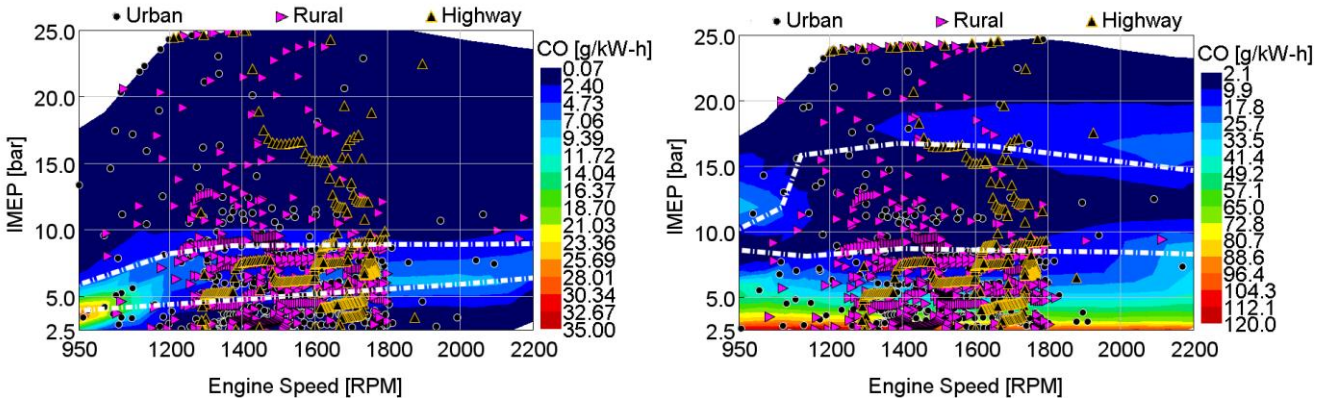

Figure 11. Operation points in CO emission map for RCCI/CDC concept (left) and DMDF concept (right).

Operating points in soot emission maps present similar values for both concepts due to the fact that most of the operating points are in the low emission region. However, an inversion is observed in the red zone of the DMDF map (Figure 12), where diffusive combustion prevails, showing higher soot emissions at high engine speeds and loads. On the other hand, for RCCI/CDC the highest values occur at intermediate engine speeds and low loads. An increase of 0.002 g/kWh of soot is observed for RCCI/CDC if compared to the values obtained with DMDF combustion strategy.

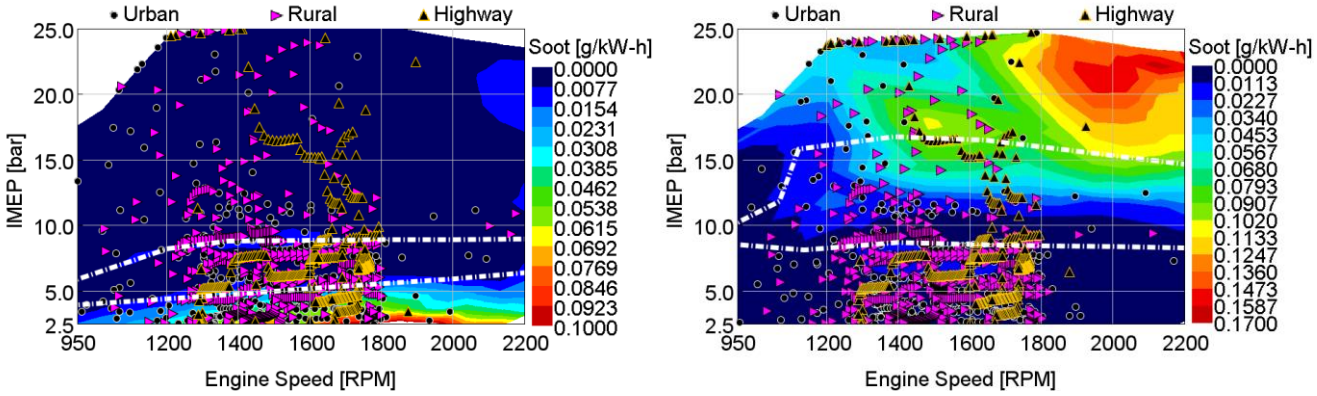

Figure 12. Operation points in Soot emission map for RCCI/CDC concept (left) and DMDF concept (right).

Figure 13 to Figure 18 present the gasoline substitution rates (E20-95 in RCCI/CDC mode and 95 RON gasoline in DMDF), total fuel consumption and emissions rates during the three segments of WHVC driving cycle. The vehicle speed profile in each phase is included in the upside part of the plots. According to Figure 13, the average fuel consumption for both concepts is higher in the highway segment due to few decelerations and stops (low loads). Despite the similar values, fuel consumption of three segments is lower for DMDF concept. The right side of Figure 13 points to the total mass of fuel consumed during the cycle and to the respective gasoline portion. The difference between these values represents the diesel fuel mass consumed. As it can be seen, although DMDF consumes greater mass of gasoline, the total fuel mass (diesel+gasoline) is lower when compared to the RCCI/CDC concept, leading to a fuel

consumption decrease of 7% at the end of the cycle. This can be explained by the larger portion of the map covered by RCCI regime.

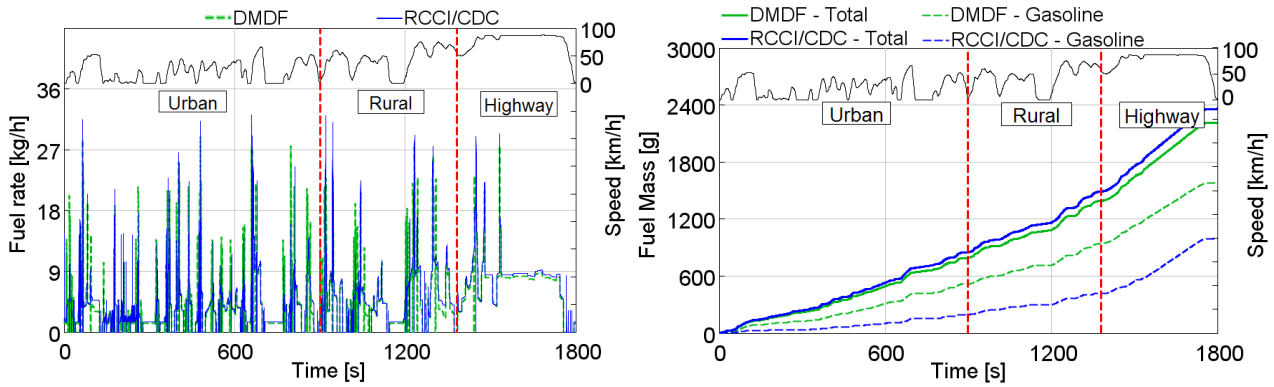

Figure 13. Instantaneous fuel rate (left) and cumulative fuel mass (right) in WHVC driving cycle.

The difference in drive cycle NO_x emissions for both concepts showed in Figure 9 shows highest average NO_x emission rate of RCCI/CDC in the rural segment (52 g/h), followed by urban (43 g/h) and highway cycle (34 g/h). In Figure 14, peaks in the instantaneous NO_x emission rate can be observed during rapid accelerations, yielding values greater than 1400 g/h. For DMDF, these peaks are not observed, contributing to the significant reduction in the average NO_x emissions of each segment, 5 g/h for urban, 8 g/h for rural and 9 g/h for the highway portion.

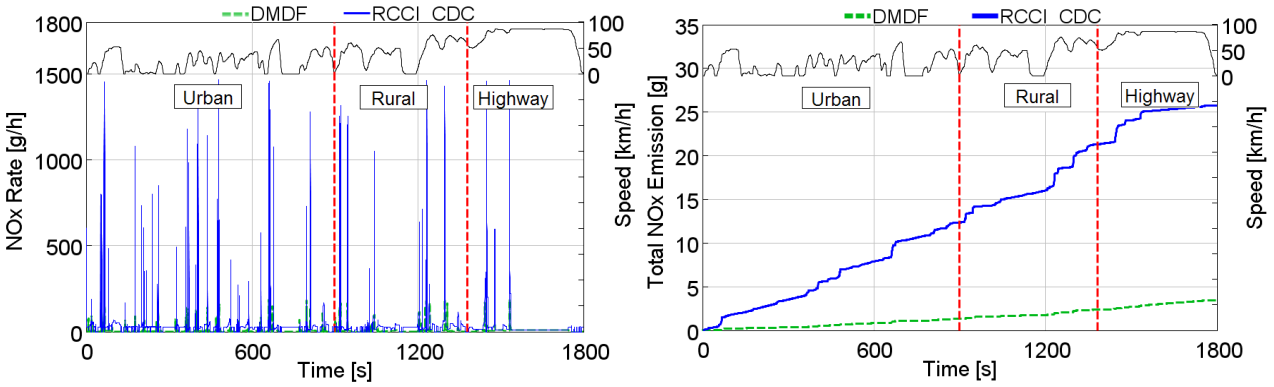

Figure 14. Instantaneous NO_x emission rate (left) and cumulative NO_x emission mass (right) in WHVC driving cycle.

According to Figure 15, the trend of HC emissions is similar to that observed for fuel consumption, being greater in highway conditions. However, peaks of emissions in instantaneous accelerations are not so representative in the total average. RCCI/CDC presented lower values at all stages when compared to DMDF combustion concept.

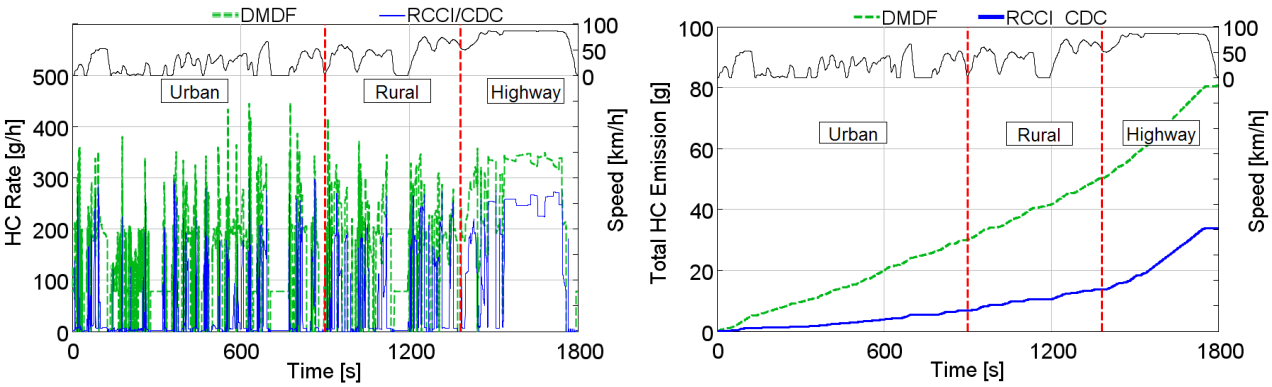

Figure 15. Instantaneous HC emission rate (left) and cumulative HC emission mass (right) in WHVC driving cycle.

Figure 16 shows the significantly higher values of instantaneous CO emissions for DMDF throughout the driving cycle. The difference observed in the maps of Figure 11 justifies that greater values of average CO emission for DMDF are in urban conditions, where the engine operates in low loads. For the RCCI/CDC concept, greater CO emissions are observed in highway condition which subjects the engine to moderate loads.

Prikhodko et al. [43] demonstrated that conventional Diesel Oxidation Catalysts (DOCs) are effective in oxidizing CO and HC from RCCI operation at temperatures greater than 300°C. Considering the experimental exhaust temperature reported in previous works [31][32], rural and highway driving conditions are expected to provide enough exhaust temperature for an effective DOC operation, thus lowering CO and HC emissions under the EURO VI levels. However, HC and CO emissions in the urban area are expected to be very high, pointing out the necessity of investigating dedicated DOC technologies for this dual-mode concept.

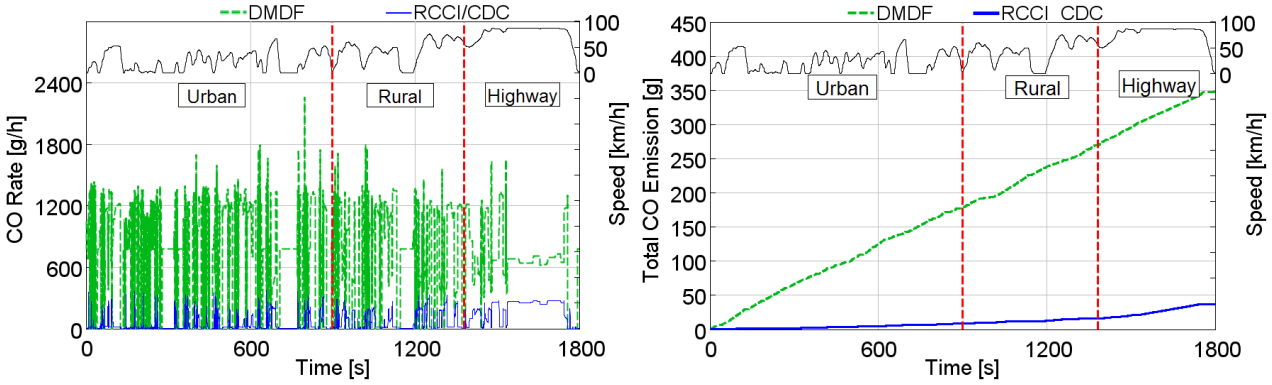

Figure 16. Instantaneous CO emission rate (left) and cumulative CO emission mass (right) in WHVC driving cycle.

The moderate engine loads in highway conditions results in the segment with greater soot emission rate for DMDF concept, being the average rate twice as high in highway segment as in the urban segment. Total average soot emission rate is 0.04 g/h lower using the RCCI/CDC strategy if compared to the DMDF strategy.

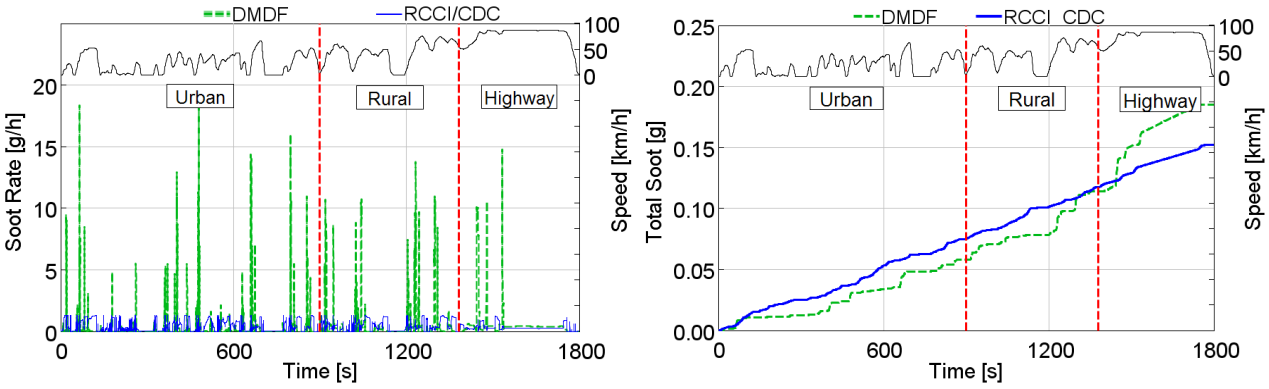

Figure 17. Instantaneous Soot emission rate (left) and cumulative Soot emission mass (right) in WHVC driving cycle.

Complementing Figure 13, Figure 18 shows the gasoline fraction as a percentage of total fuel consumed during the cycle. DMDF model presents operating points using more than 95% of gasoline and then less than 5% of diesel. Thus, despite of RCCI/CDC operation with replacements of up to 80% of gasoline in some parts of the map, more than 56% of the driving cycle is covered by CDC combustion, which leads to a substantially lower total substitution rate.

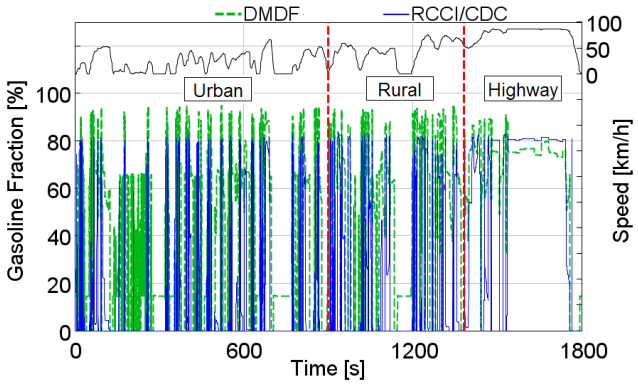

Figure 18. Instantaneous gasoline fraction for DMDF concept and RCCI/CDC concept in WHVC driving cycle.

Finally, a comparison of raw simulated values between both dual-mode concepts is shown in table 7. The EURO VI requirements of specific emissions for diesel heavy-duty vehicles is included as reference [35]. The reduction on NO_x is one of the greatest advantages of using DMDF. On the other hand, this concept presents higher values for CO and HC emissions, which shows the need of an aftertreatment system to meet this standard. Despite the better values of CO and HC emissions, RCCI/CDC concept requires more than 3 g/km of urea to reduce NO_x to EURO VI levels (in conditions of WHVC driving cycle), thus requiring a specific aftertreatment system.

Table 7. Emissions and fuel consumption comparison between both dual-mode concepts. EURO VI limits are included as reference.

	EURO VI	RCCI/CDC	DMDF
BSCO [g/kWh]	4.00	3.64	33.67
BSHC [g/kWh]	0.16	3.31	7.79
BSNO_x [g/kWh]	0.46	2.52	0.33
BSSoot [g/kWh]	0.01	0.015	0.018
BSFC [g/kWh]	-	230.17	213.87

4. Conclusions

The present work has evaluated the emissions and performance of two dual-mode RCCI combustion strategies under the WHVC. For this purpose, a one dimensional vehicle model of a Volvo FL240 truck was developed with GT-Suite. Experimental emissions and fuel consumption data used as inputs for running the WHVC driving cycle simulations were acquired experimentally on the actual medium-duty engine used in the FL240 truck.

The analysis of the effect of seven different gear shifting strategies on the engine-out emissions and performance showed that the gear shifting strategy that covers the range of maximum engine torque (1200-1800 rpm) leads to the lowest fuel consumption with balanced engine-out emissions for both dual-mode concepts, DMDF and RCCI/CDC. By this reason, this gear shifting strategy was selected for performing a detailed comparison between both dual-mode combustion strategies.

The direct comparison of both dual-mode concepts using the optimal gear shifting strategy revealed that dual-mode dual-fuel (DMDF) concept allows reducing the specific fuel consumption by 7% in average in comparison to RCCI/CDC concept. Moreover, NO_x emissions are around 87% lower with dual-mode dual-fuel, meeting the EURO VI requirements without the need for an SCR aftertreatment system. On the other hand, HC and CO emissions are near 2 and 10 times greater, respectively, for dual-mode dual-fuel than for RCCI/CDC. This points out the need for studying the efficiency of the DOC catalytic systems in oxidizing HC and CO emissions from dual-fuel dual mode in transient conditions.

Acknowledgments

The experimental results used in this work come from an investigation funded by VOLVO Group Trucks Technology. The authors also acknowledge the Spanish economy and competitiveness ministry for partially supporting this research (HiReCo TRA2014-58870-R). The author J. Monsalve-Serrano acknowledges the financial support from the Universitat Politècnica de València under the Grant “Ayudas Para la Contratación de Doctores para el Acceso al Sistema Español de Ciencia, Tecnología e Innovación”.

The author Vinícius Rückert Roso would like to acknowledge the financial support from CAPES in providing the necessary bursary and to the Universidade Federal de Santa Maria and Universidade Federal de Minas Gerais-Brazil by the financial support in acquiring the software licenses needed for this work.

References

[1] The European Commission. Energy, Transport and Environment Indicators. Technical report, 2014.

[2] Dhinesh B, Annamalai M, Isaac JoshuaRamesh Lalvani J, Annamalai K. Studies on the influence of combustion bowl modification for the operation of Cymbopogon Flexuosus biofuel based diesel blends in a DI diesel engine. Applied Thermal Engineering112 (2017) 627-637.

[3] Dhinesh B, Isaac JoshuaRamesh Lalvani J, Parthasarathy M, Annamalai K. An assessment on performance, emission and combustion characteristics of single cylinder diesel engine powered by Cymbopogon flexuosus biofuel. Energy Conversion and Management 117 (2016) 466-474.

[4] Annamalai M, Dhinesh B, Nanthagopal K, SivaramaKrishnan P, Isaac JoshuaRamesh Lalvani J, Parthasarathy M, Annamalai K. An assessment on performance, combustion and emission behavior of a diesel engine powered by ceria nanoparticle blended emulsified biofuel. Energy Conversion and Management 123 (2016) 372-380.

[5] Garcia A, Monsalve-Serrano J, Heuser B, Jakob M, Kremer F, Pischinger S. Influence of fuel properties on fundamental spray characteristics and soot emissions using different tailor-made fuels from biomass. Energy Conversion and Management, Volume 108, 15 January 2016, Pages 243-254.

[6] Engineer Commercial Vehicle. Euro 6 the inside story. Technical report, March 2012.

[7] Johnson TV. Vehicular Emissions in Review. SAE Int. J. Engines, Vol. 7, pp. 1207-1227, 2014.

[8] Posada F, Chambliss S, Blumberg K. Costs of emission reduction technologies for heavy-duty diesel vehicles. ICCT White paper, 2016.

[9] Shi L, Deng K, Cui Y, Qu S, Hu W. Study on knocking combustion in a diesel HCCI engine with fuel injection in negative valve overlap. Fuel, Volume 106, April 2013, Pages 478–483.

[10] Ahmedi A, Ahmed SS, Kalghatgi GT. Simulating combustion in a PCI (premixed compression ignition) engine using DI-SRM and 3 components surrogate model. Combustion and Flame, Volume 162, Issue 10, 2015, Pages 3728-3739.

[11] Jain A, Singh A, Agarwal A. Effect of fuel injection parameters on combustion stability and emissions of a mineral diesel fueled partially premixed charge compression ignition (PCCI) engine. Applied Energy, Volume 190, 15 March 2017, Pages 658-669.

[12] Leermakers C, Bakker P, Nijssen B, Somers L, Johansson B. Low octane fuel composition effects on the load range capability of partially premixed combustion. Fuel, Volume 135, 1 November 2014, Pages 210-222.

[13] Benajes J, Molina S, García A, Monsalve-Serrano J, Durrett R. Conceptual model description of the double injection strategy applied to the gasoline partially premixed compression ignition combustion concept with spark assistance. Applied Energy, Volume 129, 15 September 2014, Pages 1-9.

[14] Benajes J, Molina S, García A, Monsalve-Serrano J, Durrett R. Performance and engine-out emissions evaluation of the double injection strategy applied to the gasoline partially premixed compression ignition spark assisted combustion concept. Applied Energy, Volume 134, 1 December 2014, Pages 90-101.

[15] Kokjohn S L, Hanson R M, Splitter D A, Reitz R D. Fuel reactivity controlled compression ignition (RCCI): a pathway to controlled high-efficiency clean combustion, International Journal of Engine Research, 2011. Volume 12, June 2011, Pages 209-226.

[16] Inagaki K, Fuyuto T, Nishikawa K, Nakakita K, Sakata I. Dual-fuel PCI combustion controlled by in-cylinder stratification of ignitability. SAE technical paper 2006-01-0028, 2006.

[17] Desantes JM, Benajes J, García A, Monsalve-Serrano J. The Role of the In-Cylinder Gas Temperature and Oxygen Concentration over Low Load RCCI Combustion Efficiency. Energy, Volume 78, 15 December 2014, Pages 854-868.

[18] Benajes J, García A, Monsalve-Serrano J, Boronat V. Dual-Fuel Combustion for Future Clean and Efficient Compression Ignition Engines. Applied Sciences 7(1):36, 2017.

[19] Benajes J, Pastor JV, García A, Monsalve-Serrano J. The potential of RCCI concept to meet EURO VI NO_x limitation and ultra-low soot emissions in a heavy-duty engine over the whole engine map. Fuel, Volume 159, November 2015, Pages 952–961.

[20] Benajes J, García A, Monsalve-Serrano J, Boronat V. Gaseous emissions and particle size distribution of dual-mode dual-fuel diesel-gasoline concept from low to full load. Applied Thermal Engineering, Volume 120, 25 Jun 2017, Pages 138-149.

[21] Nazemi M, Shahbakhti M. Modeling and analysis of fuel injection parameters for combustion and performance of an RCCI engine. Applied Energy, Vol. 165, pp 135-150, 2016.

[22] Benajes J, Molina S, García A, Monsalve-Serrano J. Effects of Direct injection timing and Blending Ratio on RCCI combustion with different Low Reactivity Fuels. Energy Conversion and Management, Volume 99, 15 July 2015, Pages 193-209.

[23] Li J, Yang WM, Zhou DZ. Modeling study on the effect of piston bowl geometries in a gasoline/biodiesel fueled RCCI engine at high speed. Energy Conversion and Management, Volume 112, 2016, Pages 359-368.

[24] Benajes J, Pastor JV, García A, Boronat V. A RCCI operational limits assessment in a medium duty compression ignition engine using an adapted compression ratio. Energy Conversion and Management, Volume 126, 2016, Pages 497-508.

[25] Fang W, Kittelson D, Northrop W. Optimization of reactivity-controlled compression ignition combustion fueled with diesel and hydrous ethanol using response surface methodology. Fuel, Volume 160, 2015, Pages 446-457.

[26] Benajes J, Molina S, García A, Monsalve-Serrano J. Effects of low reactivity fuel characteristics and blending ratio on low load RCCI (reactivity controlled compression ignition) performance and emissions in a heavy-duty diesel engine. Energy, Volume 90, October 2015, Pages 1261-1271.

[27] Splitter D, Wissink M, DelVescovo D, Reitz R. RCCI Engine Operation Towards 60% Thermal Efficiency. SAE Technical Paper 2013-01-0279, 2013, doi:10.4271/2013-01-0279.

[28] Li Y, Jia M, Chang Y, Fan W, Xie M, Wang T. Evaluation of the necessity of exhaust gas recirculation employment for a methanol/diesel reactivity controlled compression ignition engine operated at medium loads. Energy Conversion and Management, Volume 101, 2015, Pages 40-51.

[29] Benajes J, García A, Monsalve-Serrano J, Boronat V. An investigation on the particulate number and size distributions over the whole engine map from an optimized combustion strategy combining RCCI and dual-fuel diesel-gasoline. Energy Conversion and Management, Volume 140, 15 May 2017, Pages 98-108.

[30] Benajes J, García A, Monsalve-Serrano J, Balloul I, Pradel G. Evaluating the reactivity controlled compression ignition operating range limits in a high-compression ratio medium-duty diesel engine fueled with biodiesel and ethanol. International Journal of Engine Research, Volume 18 (1-2), Pages 66-80, 2017.

[31] Benajes J, García A, Monsalve-Serrano J, Balloul I, Pradel G. An assessment of the dual-mode reactivity controlled compression ignition/conventional diesel combustion capabilities in a EURO VI medium-duty diesel engine fueled with an intermediate ethanol-gasoline blend and biodiesel. Energy Conversion and Management, Volume 123, July 2016, Pages 381-391.

[32] Benajes J, García A, Monsalve-Serrano J, Boronat V. Achieving clean and efficient engine operation up to full load by combining optimized RCCI and dual-fuel diesel-gasoline combustion strategies. Energy Conversion and Management, Volume 136, 15 March 2017, Pages 142-151.

[33] Banjac T, Trenc F, Katrašnik T. Energy conversion efficiency of hybrid electric heavy-duty vehicles operating according to diverse drive cycles. Energy Conversion and Management, Volume 50, Issue 12, December 2009, Pages 2865-2878.

[34] Smith I, Briggs T, Sharp C, Webb C. Achieving 0.02 g/bhp-hr NO_x Emissions from a Heavy-Duty Stoichiometric Natural Gas Engine Equipped with Three-Way Catalyst. SAE Technical Paper 2017-01-0957, 2017, doi:10.4271/2017-01-0957.

[35] Regulation (EC) No 595/2009 of the European Parliament and of the Council on type-approval of motor vehicles and engines with respect to emissions from heavy duty vehicles (Euro VI). http://eur-lex.europa.eu.

[36] Benajes J, Pastor JV, García A, Monsalve-Serrano J. An experimental investigation on the Influence of piston bowl geometry on RCCI performance and emissions in a heavy-duty engine. Energy Conversion and Management, Volume 103, October 2015, Pages 1019-1030.

[37] Benajes J, García A, Pastor JM, Monsalve-Serrano J. Effects of piston bowl geometry on Reactivity Controlled Compression Ignition heat transfer and combustion losses at different engine loads. Energy, Volume 98, March 2016, Pages 64-77.

[38] GT-Suite. Engine Performance Application Manual. 7.6. 2016.

[39] Grigoratos T. Fontaras G. Martini G. Peletto C. A study of regulated and green house gas emissions from a prototype heavy-duty compressed natural gas engine under transient and real life conditions. Energy. Volume 103. March 2016. Pages 340-355.

[40] Fontaras G. Grigoratos T. Savvidis D. Anagnostopoulos K. Luz R. Rexeis M. Hausberger S. An experimental evaluation of the methodology proposed for the monitoring and certification of CO2 emissions from heavy-duty vehicles in Europe. Energy. Volume 102. March 2016. Pages 354-364.

[41] www.volvotrucks.co.uk/en-gb/trucks/volvo-fl/specifications/driveline.html

[42] Johnson T. Diesel emissions in review. SAE Int J Engines 2011;4(1):143-57. http://dx.doi.org/10.4271/2011-01-0304.

[43] Prikhodko V. Curran S. Parks J. Wagner R. Effectiveness of diesel oxidation catalyst in reducing HC and CO emissions from reactivity controlled compression ignition. SAE Int J Fuels Lubr 2013;6(2):329–35. http://dx.doi.org/10.4271/2013-01-0515.

Abbreviations

ATDC: After Top Dead Center

BMEP: Brake Mean Effective Pressure

BSFC: Brake Specific Fuel Consumption

B7: Diesel fuel with 7% of biodiesel content by volume

CAD: Crank Angle Degree

CDC: Conventional Diesel Combustion

CI: Compression Ignition

CO: Carbon Monoxide

CR: Compression Ratio

DOC: Diesel Oxidation Catalyst

DMDF: Dual-Mode Dual-Fuel

DPF: Diesel Particulate Filter

ECU: Electronic Control Unit

EGR: Exhaust Gas Recirculation

EU: European Union

E20-95: Fuel blend of 95 ON gasoline and 20% of ethanol by volume

FSN: Filter Smoke Number

GIE: Gross Indicated Efficiency

HC: Hydro Carbons

HCCI: Homogeneous Charge Compression Ignition

IMEP: Indicated Mean Effective Pressure

ICE: Internal Combustion Engines

IVC: Intake Valve Close

IVO: Intake Valve Open

LRF: Low Reactivity Fuel

LTC: Low Temperature Combustion

MON: Motor Octane Number

PCI: Premixed Compression Ignition

PFI: Port Fuel Injection

PPC: Partially Premixed Charge

PRR: Pressure Rise Rate

RON: Research Octane Number

RCCI: Reactivity Controlled Compression Ignition

SI: Spark ignition

SCE: Single Cylinder Engine

SCR: Selective Catalytic Reduction

TDC: Tope Dead Center

WHTC: World Harmonized Transient Cycle

WHVC: World Harmonized Vehicle Cycle